



## Measurement of the $W$ boson helicity in top quark decays at DØ

(DØ Collaboration)

(Dated: July 18, 2007)

We present a measurement of the helicity of  $W$  bosons produced in top quark decays, based on a candidate sample of  $t\bar{t}$  events in the  $\ell$ +jets and dilepton decay channels corresponding to an integrated luminosity of  $1 \text{ fb}^{-1}$  collected by the DØ detector at the Fermilab Tevatron  $p\bar{p}$  Collider at  $\sqrt{s} = 1.96 \text{ TeV}$ . We reconstruct the decay angle  $\theta^*$  for each lepton. A fit with  $f_0$  fixed to the standard model value yields  $f_+ = 0.017 \pm 0.048 \text{ (stat)} \pm 0.047 \text{ (syst)}$ . ( $f_+ < 0.14$  at 95% C.L.), consistent with the standard model prediction of  $f_+ = 3.6 \times 10^{-4}$ .

The top quark is by far the heaviest of the known fermions and is the only one that has a Yukawa coupling of order unity to the Higgs boson in the standard model. In the standard model, the top quark decays via the  $V - A$  charged current interaction, almost always to a  $W$  boson and a  $b$  quark. We search for evidence of new physics in  $t \rightarrow Wb$  decay by measuring the helicity of the  $W$  boson. A different form for the  $t \rightarrow Wb$  coupling would alter the fractions of  $W$  bosons produced in each of the three possible polarization states. For any linear combination of  $V$  and  $A$  currents at the  $t \rightarrow Wb$  vertex, the fraction  $f_0$  of longitudinally-polarized  $W$  bosons is  $0.697 \pm 0.012$  [1] at the world average top quark mass  $m_t$  of  $172.5 \pm 2.3 \text{ GeV}$  [2].

In this analysis, we consider only linear combinations of  $V + A$  and  $V - A$  couplings, which means that we fix  $f_0 = 0.70$  and measure the positive helicity fraction  $f_+$ . In the standard model,  $f_+$  is predicted to be  $3.6 \times 10^{-4}$  [3] at next-to-leading order. A measurement of the  $f_+$  that differs significantly from the standard model value would be an unambiguous indication of new physics.

Measurements of the  $b \rightarrow s\gamma$  decay rate have indirectly limited the  $V + A$  contribution in top quark decays to less than a few percent [4]. Direct measurements of the  $V + A$  contribution are still necessary because the limit from  $b \rightarrow s\gamma$  assumes that the electroweak penguin contribution is dominant. Direct measurements of the longitudinal fraction (in which  $f_+$  is set to zero) found  $f_0 = 0.91 \pm 0.39$  [5],  $f_0 = 0.56 \pm 0.31$  [6], and  $f_0 = 0.61 \pm 0.13$  [7]. Direct measurements of  $f_+$  (in which  $f_0$  is set to 0.7) have found  $f_+ = -0.02 \pm 0.07$  ( $f_+ < 0.09$  at 95% C.L.) [8], and  $f_+ = 0.056 \pm 0.098$  ( $f_+ < 0.23$  at 95% C.L.) [9]. The analysis presented in this article improves upon that reported in Ref. [9] by using a larger data set, and employing enhanced event selection techniques.

The angular distribution of the down-type decay products of the  $W$  boson (charged lepton or  $d$ ,  $s$  quark) in the rest frame of the  $W$  boson can be described by introducing the decay angle  $\theta^*$  of the down-type particle with respect to the top quark direction. The dependence of the distribution of  $\cos \theta^*$  on the  $W$  boson helicity fractions,

$$\omega(c_{\theta^*}) \propto 2(1 - c_{\theta^*}^2)f_0 + (1 - c_{\theta^*})^2f_- + (1 + c_{\theta^*})^2f_+, \quad (1)$$

where  $f_+$ ,  $f_0$ , and  $f_-$  must sum to one and  $c_{\theta^*} = \cos \theta^*$ , forms the basis for our measurement. We proceed by selecting a data sample enriched in  $t\bar{t}$  events, reconstructing the four vectors of the two top quarks and their decay products (the top quark mass is taken to be  $172.5 \text{ GeV}$ ), and then calculating  $\cos \theta^*$ . This distribution in  $\cos \theta^*$  is compared with templates for different  $W$  boson helicity models, suitably corrected for background and reconstruction effects, using a binned maximum likelihood method. In the  $\ell$ +jets channel, the kinematic reconstruction is done with a fit that constrains the  $W$  boson mass to its measured value, while in the dilepton channel, the kinematics are solved algebraically.

The DØ detector [10] comprises three main systems: the central tracking system, the calorimeters, and the muon system. The central-tracking system is located within a 2 T solenoidal magnet. The next layer of detection involves three liquid-argon/uranium calorimeters: a central section covering pseudorapidities [11]  $|\eta| \lesssim 1$ , and two end calorimeters extending coverage to  $|\eta| \approx 4$ , all housed in separate cryostats. The muon system is located outside the calorimetry, and consists of a layer of tracking detectors and scintillation trigger counters before 1.8 T iron toroids, followed by two similar layers after the toroids.

This measurement uses a data sample recorded with the DØ experiment that corresponds to an integrated luminosity of about  $1 \text{ fb}^{-1}$  of  $p\bar{p}$  collisions at  $\sqrt{s} = 1.96 \text{ TeV}$ . The data sample consists of  $t\bar{t}$  candidate events from the  $\ell$ +jets decay channel

$t\bar{t} \rightarrow W^+W^-b\bar{b} \rightarrow \ell\nu qq'\bar{b}\bar{b}$  and the dilepton channel  $t\bar{t} \rightarrow W^+W^-b\bar{b} \rightarrow \ell\nu\ell'\nu'\bar{b}\bar{b}$ , where  $\ell$  and  $\ell'$  are electrons or muons. The  $\ell$ +jets final state is characterized by one charged lepton, at least four jets, and significant missing transverse energy ( $\cancel{E}_T$ ). The dilepton final state is characterized by two charged leptons of opposite sign, at least two jets, and significant  $\cancel{E}_T$ . In both final states, at two of the jets are  $b$  jets.

We simulate  $t\bar{t}$  signal events with  $m_t = 172.5$  GeV for different values of  $f_+$  with the ALPGEN Monte Carlo (MC) program [12] for the parton-level process (leading order) and PYTHIA [13] for gluon radiation and subsequent hadronization. As the interference term between  $V - A$  and  $V + A$  is suppressed by the small mass of the  $b$  quark and is therefore negligible [14], samples with  $f_+ = 0.00$  and  $f_+ = 0.30$  are used to create  $\cos\theta^*$  templates for any  $f_+$  value by a linear interpolation of the templates. The MC samples used to model background events with real leptons are also generated using ALPGEN and PYTHIA.

The  $\ell$ +jets event selection [15] requires an isolated lepton ( $e$  or  $\mu$ ) with transverse momentum  $p_T > 20$  GeV, no other lepton with  $p_T > 15$  GeV in the event,  $\cancel{E}_T > 20$  GeV, and at least four jets. Electrons are required to have  $|\eta| < 1.1$  and are identified by their energy deposition and isolation in the calorimeter, their transverse and longitudinal shower shapes, and information from the tracking system. Also, a discriminant combining the above information must be consistent with the expectation for a high- $p_T$  isolated electron [15]. Muons are identified using information from the muon and tracking systems, and must satisfy isolation requirements based on the energies of calorimeter clusters and the momenta of tracks around the muon. They are required to have  $|\eta| < 2.0$  and to be isolated from jets. Jets are reconstructed using the Run II mid-point cone algorithm with cone radius 0.5 [16], and are required to have rapidity  $|y| < 2.5$  and  $p_T > 20$  GeV.

Backgrounds in the  $\ell$ +jets channel arise predominantly from  $W$ +jets production and multijet production where one of the jets is misidentified as a lepton and spurious  $\cancel{E}_T$  appears due to mismeasurement of the transverse energy in the event. We determine the number of multijet background events  $N_{mj}$  from the data, using the technique described in Ref. [15]. We calculate  $N_{mj}$  for each bin in the  $\cos\theta^*$  distribution from the data sample to obtain the multijet  $\cos\theta^*$  templates.

In the dilepton channel, backgrounds arise from processes such as  $WW$ +jets or  $Z$ +jets. Events are required to have two leptons with opposite charge and  $p_T > 15$  GeV and two or more jets with  $p_T > 20$  GeV and  $|y| < 2.5$ .

To further refine the sample following the above selection, a likelihood discriminant  $\mathcal{D}$  with values in the range 0 to 1 is calculated using input variables which exploit differences in kinematics and jet flavor. The kinematic variables considered are:  $H_T$  (defined as the scalar sum of the jet  $p_T$  values), centrality (the ratio of  $H_T$  to the sum of the jet energies),  $k'_{Tmin}$  (the distance in  $\eta - \phi$  space between the closest pair of jets multiplied by the  $E_T$  of the lowest- $E_T$  jet in the pair, and divided by the  $E_T$  of the  $W$ ), the sum of all jet and charged lepton energies  $h$ , the minimum dijet mass of the jet pairs  $m_{jjmin}$ , aplanarity  $\mathcal{A}$ , and sphericity  $\mathcal{S}$  [17]. In the dilepton channels the missing  $\cancel{E}_T$  and dilepton invariant mass  $m_{\ell\ell}$  are also used. In the dimuon channel the  $\chi^2$  of a kinematic fit to the  $Z \rightarrow \mu\mu$  hypothesis  $\chi_Z^2$  is used instead of  $\cancel{E}_T$ .

We utilize the fact that background jets arise mostly from light quarks or gluons while two of the jets in  $t\bar{t}$  events arise from  $b$  quarks by forming a neural network discriminant between  $b$  and light jets. Inputs to this neural network include track impact parameters and the properties of any secondary decay vertices reconstructed within the jet cone, and the output is a value  $NN_b$  that is near one for  $b$  jets and near zero for light jets. In the  $\ell$ +jets channels we use the average of the two largest  $NN_b$  values to form a continuous variable  $\langle NN_b \rangle$  that tends to be large for  $t\bar{t}$  events and small for backgrounds, while in the dilepton channels the  $NN_b$  values for the two leading jets ( $NN_1, NN_2$ ) are taken as separate variables. Including  $NN_b$  as a continuous variable in the discriminant results in similar background discrimination but better efficiency than applying a simple cut on  $NN_b$ .

The discriminant is built separately for each of the five final states considered, using the method described in Refs. [15, 18]. Background events tend to have  $\mathcal{D}$  values near 0, while  $t\bar{t}$  events tend to have values near 1. We consider all possible combinations of the above variables for use in the discriminant, and all possible requirements on the  $\mathcal{D}$  value, and choose the variables and  $\mathcal{D}$  criterion that give the smallest expected uncertainty on  $f_+$ . The variables used, and the requirement placed on  $\mathcal{D}$  for each channel, are given in Table I.

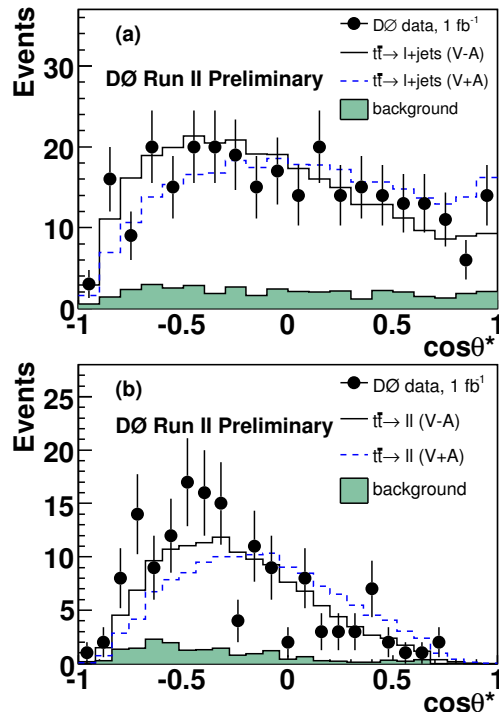
We then perform a binned Poisson maximum likelihood fit to compare the observed distribution of events in  $\mathcal{D}$  to the sum of the distributions expected from  $t\bar{t}$  and background events. In the  $\ell$ +jets channels  $N_{mj}$  is constrained to the expected value within the known uncertainty, while in the dilepton channels the ratio of the various background sources is fixed to the expectation from the cross sections times efficiency of the kinematic selection. The likelihood is then maximized with respect to the numbers of  $t\bar{t}$ , and background events, which are multiplied by the appropriate efficiency for the  $\mathcal{D}$  selection to determine the composition of the sample used for measuring  $\cos\theta^*$ . Table I lists the composition of each sample as well as the number of observed events in the data.

The top quark and  $W$  boson four-momenta in the selected  $\ell$ +jets events are reconstructed using a kinematic fit which is subject to the following constraints: two jets must form the invariant mass of the  $W$  boson, the lepton and the  $\cancel{E}_T$  together with the neutrino  $p_z$  component must form the invariant mass of the  $W$  boson, and the masses of the two reconstructed top quarks must be 172.5 GeV. Among the twelve possible jet combinations, the solution with the maximal probability, considering both the  $\chi^2$  from the kinematic fit and the  $NN_b$  values of the four jets, is chosen; MC studies show this selects the jet that originated from the leptonically-decaying top quark in about 70% of all cases. The  $\cos\theta^*$  distribution obtained in the  $\ell$ +jets data after the full selection and compared to standard and  $V + A$  model expectations is shown in Fig. 1(a).

Dilepton events are rarer than  $\ell$ +jets events, but have the advantage that  $\cos\theta^*$  can be calculated for each lepton, thus providing two measurements per event. The presence of two neutrinos in the dilepton final state makes the system kinematically

TABLE I: Summary of the event selection and number of selected events for each of the  $t\bar{t}$  final states used in this analysis.

	$e+\text{jets}$	$\mu+\text{jets}$	$e\mu$	$ee$	$\mu\mu$
Variables used in discriminant $\mathcal{D}$	$\mathcal{C}, \mathcal{S}, \mathcal{A}, H_T, h, k'_{Tmin}, \langle NN_b \rangle$	$\mathcal{C}, \mathcal{S}, H_T, k'_{Tmin}, \langle NN_b \rangle$	$\mathcal{C}, \mathcal{S}, h, m_{jj}, k'_{Tmin}, NN_1, NN_2$	$\mathcal{A}, \mathcal{S}, k'_{Tmin}, \cancel{E}_T, NN_1, m_{\ell\ell}$	$\mathcal{A}, \mathcal{S}, h, m_{jj}, \chi_Z^2, NN_1, m_{\ell\ell}$
Signal before $\mathcal{D}$ selection	$131.0 \pm 13.9$	$156.0 \pm 14.9$	$41.7 \pm 7.1$	$18.1 \pm 5.4$	$42 \pm 11$
Background before $\mathcal{D}$ selection	$217.4 \pm 18.9$	$201.0 \pm 19.3$	$21.3 \pm 5.4$	$1258 \pm 36$	$1728 \pm 43$
Data events before $\mathcal{D}$ selection	347	355	63	1276	1770
Requirement on $\mathcal{D}$	$> 0.80$	$> 0.40$	$> 0.08$	$> 0.986$	$> 0.990$
Background after $\mathcal{D}$ selection	$21.1 \pm 4.5$	$33.0 \pm 5.2$	$9.9 \pm 2.5$	$2.2 \pm 0.9$	$4.8 \pm 3.4$
Data events after $\mathcal{D}$ selection	121	167	45	15	15

FIG. 1:  $\cos \theta^*$  distribution observed in (a)  $\ell+\text{jets}$  and (b) dilepton events. The standard model prediction is shown as the solid line, while a model with a pure  $V + A$  interaction would result in the distribution given by the dashed line.

underconstrained. However, if a top quark mass is assumed, the kinematics can be solved algebraically with a four-fold ambiguity in addition to the two-fold ambiguity in pairing jets with leptons. For each lepton, we calculate the value of  $\cos \theta^*$  resulting from each solution with each of the two leading jets associated with the lepton. To account for detector resolution we repeat the above procedure 500 times, fluctuating the jet and lepton energies within their resolutions for each iteration. The average of these values is taken as the  $\cos \theta^*$  for that lepton. The  $\cos \theta^*$  distribution obtained in dilepton data is shown in Fig. 1(b).

We compute the binned Poisson likelihood  $L(f_+)$  for the data to be consistent with the sum of signal and background templates at each of seven chosen  $f_+$  values. The background normalization is constrained to be consistent within errors with the expected value by a Gaussian term in the likelihood. A parabola is fit to the  $-\ln[L(f_+)]$  points to determine the likelihood as a function of  $f_+$ . This fit is done separately for the  $\ell+\text{jets}$  and dilepton channels, and the results are combined by summing the  $-\ln[L(f_+)]$  points.

Systematic uncertainties are evaluated in ensemble tests by varying the parameters that can affect the shapes of the  $\cos \theta^*$  distributions or the relative contribution from signal and background sources. Ensembles are formed by drawing events from a model with the parameter under study varied. These are compared to the standard  $\cos \theta^*$  templates in a maximum likelihood fit. The average shift in the resulting  $f_+$  values are taken as the systematic uncertainty and is shown in Table II. The total systematic uncertainty is then taken into account in the likelihood by convoluting the latter with a Gaussian with a width that corresponds to the total systematic uncertainty. The mass of the top quark is varied by  $\pm 2.3$  GeV and the jet reconstruction efficiency, energy scale, and resolution by  $\pm 1\sigma$  around their nominal values.

The statistical uncertainty on the  $\cos \theta^*$  templates is taken as a systematic uncertainty estimated by fluctuating the templates

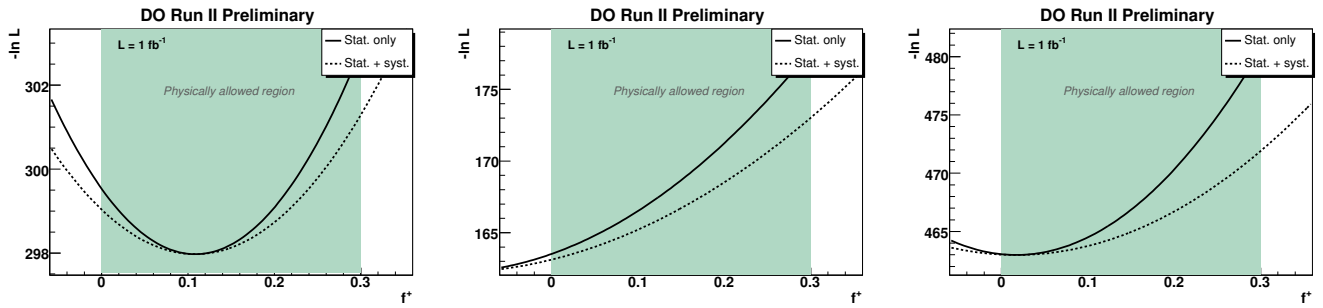


FIG. 2:  $-\ln L$  curve obtained in the (left)  $\ell$ +jets channel, (center) dilepton channel, and (right)  $\ell$ +jets and dilepton channels combined. The dashed line includes only the statistical uncertainty while the solid line also includes the systematic uncertainties. The physically allowed interval of  $f_+$  is shaded.

TABLE II: Systematic uncertainties on  $f_+$  when  $f_0$  is fixed to 0.70 for the two channels and for their combination.

Source	Dilepton	$\ell$ +jets	Combined
Jet energy scale	0.019	0.017	0.018
Jet energy resolution	0.002	0.020	0.013
Top quark mass	0.021	0.020	0.020
Template statistics	0.017	0.019	0.013
$t\bar{t}$ model	0.028	0.018	0.022
Bkg. model	0.019	0.019	0.014
Heavy flavor fraction	0.014	0.019	0.017
$NN$ variable	–	0.008	0.005
$b$ fragmentation	0.009	0.009	0.009
Jet ID	0.008	0.008	0.008
Analysis self-consistency	0.006	0.002	0.004
Total			0.047

according to their statistical uncertainty, and noting the RMS of the resulting distribution when fitting to the data.

The effect of gluon radiation in the modeling of  $t\bar{t}$  events is studied with an alternate MC sample that includes  $t\bar{t}$  events generated by PYTHIA rather than ALPGEN. We also consider samples with a different model for the underlying event and ones without zero-bias events overlaid. Effects of mis-modeling the background distribution in  $\cos\theta^*$  are assessed by comparing data to the background model for events with low  $\mathcal{D}$  values. The systematic uncertainty on the jet flavor composition in the  $W$ +jets background is derived using alternate MC samples in which the fraction of  $b$  and  $c$  jets are varied by 20% about the nominal value [20]. The difference found between the input  $f_+$  value and the reconstructed  $f_+$  value in ensemble tests is taken as the systematic uncertainty on the calibration of the analysis (analysis self-consistency).

The results of the maximum likelihood fits to the  $\cos\theta^*$  distributions observed in the data are shown in Fig. 2. Assuming a fixed value of 0.70 for  $f_0$ , we find

$$f_+ = 0.108 \pm 0.061 \text{ (stat)} \pm 0.052 \text{ (syst)} \quad (2)$$

using  $\ell$ +jets events, and

$$f_+ = -0.123 \pm 0.076 \text{ (stat)} \pm 0.051 \text{ (syst)} \quad (3)$$

using dilepton events. These results are of marginal statistical consistency, differing by  $2.2\sigma$  when uncorrelated errors are considered. As this is insufficient evidence upon which to claim new physics, we proceed under the assumption that the difference arises from statistical fluctuation. Combination of these results yields

$$f_+ = 0.017 \pm 0.048 \text{ (stat)} \pm 0.047 \text{ (syst)}. \quad (4)$$

We also calculate a Bayesian confidence interval (using a flat prior distribution which is non-zero only in the physically allowed region of  $f_+ = 0.0 - 0.3$ ) which yields

$$f_+ < 0.14 \text{ at } 95\% \text{ C.L.} \quad (5)$$

Expressed as a measurement of  $f_{V+A}$ , the fractional  $V+A$  component in the  $t \rightarrow Wb$  coupling, the combined result is equivalent to:

$$f_{V+A} = 0.056 \pm 0.160 \text{ (stat)} \pm 0.156 \text{ (syst)} \quad (6)$$

or

$$f_{V+A} < 0.47 \text{ at } 95\% \text{ C.L.} \quad (7)$$

In summary, we have measured the helicity of  $W$  bosons in  $t\bar{t}$  decays in the  $\ell$ +jets and dilepton channels, and find  $f_+ = 0.017 \pm 0.048 \text{ (stat)} \pm 0.047 \text{ (syst)}$  with  $f_0$  fixed to the standard model value. This is the most precise measurement of  $f_+$  to date and is consistent with the standard model prediction of  $f_+ = 3.6 \times 10^{-4}$  [3].

We thank the staffs at Fermilab and collaborating institutions, and acknowledge support from the DOE and NSF (USA); CEA and CNRS/IN2P3 (France); FASI, Rosatom and RFBR (Russia); CAPES, CNPq, FAPERJ, FAPESP and FUNDUNESP (Brazil); DAE and DST (India); Colciencias (Colombia); CONACyT (Mexico); KRF and KOSEF (Korea); CONICET and UBACyT (Argentina); FOM (The Netherlands); PPARC (United Kingdom); MSMT (Czech Republic); CRC Program, CFI, NSERC and WestGrid Project (Canada); BMBF and DFG (Germany); SFI (Ireland); The Swedish Research Council (Sweden); Research Corporation; Alexander von Humboldt Foundation; and the Marie Curie Program.

---

[\*] On leave from IEP SAS Kosice, Slovakia.

[†] Visitor from Helsinki Institute of Physics, Helsinki, Finland.

[‡] Visitor from Lewis University, Romeoville, IL, USA

- [1] G. L. Kane, G. A. Ladinsky, and C.-P. Yuan, Phys. Rev. D **45**, 124 (1992); R. H. Dalitz and G. R. Goldstein, *ibid.*, 1531; C. A. Nelson *et al.*, Phys. Rev. D **56**, 5928 (1997).
- [2] TeVatron Electroweak Working Group, hep-ex/0603039.
- [3] M. Fischer *et al.*, Phys. Rev. D **63**, 031501(R) (2001).
- [4] K. Fujikawa and A. Yamada, Phys. Rev. D **49**, 5890 (1994); P. Cho and M. Misiak, Phys. Rev. D **49**, 5894 (1994); C. Jessop, SLAC-PUB-9610.
- [5] CDF Collaboration, T. Affolder *et al.*, Phys. Rev. Lett. **84**, 216 (2000).
- [6] DØ Collaboration, V. M. Abazov *et al.*, Phys. Lett. B **617**, 1 (2005).
- [7] CDF Collaboration, A. Abulencia *et al.*, CDF Conf. Note 8638 (2006).
- [8] CDF Collaboration, A. Abulencia *et al.*, hep-ex/0608062 (2006).
- [9] DØ Collaboration, V. M. Abazov *et al.*, Phys. Rev. D **75**, 031102(R) (2007).
- [10] DØ Collaboration, V. M. Abazov *et al.*, Nucl. Instrum. Methods A **565**, 463 (2006).
- [11] Rapidity  $y$  and pseudorapidity  $\eta$  are defined as functions of the polar angle  $\theta$  with respect to the proton beam and the parameter  $\beta$  as  $y(\theta, \beta) \equiv \frac{1}{2} \ln[(1 + \beta \cos \theta)/(1 - \beta \cos \theta)]$  and  $\eta(\theta) \equiv y(\theta, 1)$ , where  $\beta$  is the ratio of a particle's momentum to its energy.
- [12] M. L. Mangano *et al.*, JHEP **07**, 001 (2003).
- [13] T. Sjöstrand *et al.*, Comp. Phys. Commun. **135**, 238 (2001).
- [14] C.A. Nelson *et al.*, Phys. Rev. D **56**, 5928 (1997).
- [15] DØ Collaboration, V. M. Abazov *et al.*, Phys. Lett. B **626**, 45 (2005).
- [16] G.C. Blazey *et al.*, hep-ex/0005012.
- [17] V. Barger *et al.*, Phys. Rev. D **48**, 3953 (1993).
- [18] DØ Collaboration, B. Abbott *et al.*, Phys. Rev. D **58**, 052001 (1998).
- [19] DØ Collaboration, V. M. Abazov *et al.*, "Measurement of the  $t\bar{t}$  Production Cross Section in  $p\bar{p}$  Collisions Using Dilepton Events", in preparation.
- [20] DØ Collaboration, V. M. Abazov *et al.*, Phys. Lett. B **626**, 35 (2005).